Title

Inhibition of fatty acid amide hydrolase in the CNS prevents and reverses morphine tolerance in male and female mice

Journal

British Journal of Pharmacology, 177(13)

ISSN

0007-1188

Authors

Fotio, Yannick
Palese, Francesca
Tipan, Pablo Guaman
et al.

Publication Date

2020-07-01

DOI

10.1111/bph.15031

Peer reviewed

Received: 16 July 2019 | Revised: 10 February 2020 | Accepted: 12 February 2020

DOI: 10.1111/bph.15031

RESEARCH PAPER

Inhibition of fatty acid amide hydrolase in the CNS prevents and reverses morphine tolerance in male and female mice

Yannick Fotio[1] | Francesca Palese[1] | Pablo Guaman Tipan[1] | Faizy Ahmed[1,3] | Daniele Piomelli[1,2,3]

[1]Department of Anatomy and Neurobiology, School of Medicine, University of California, Irvine, Irvine, California

[2]Department of Biological Chemistry, School of Medicine, University of California, Irvine, Irvine, California

[3]Center for the Study of Cannabis, University of California, Irvine, Irvine, California

Correspondence
Daniele Piomelli, Gillespie Neuroscience Facility, Room 3101, School of Medicine, University of California, Irvine, Irvine, CA 92697-1275.
Email: piomelli@uci.edu

Funding information
NIH, Grant/Award Numbers: R42DA033683, R41DA041871-01

Background and Purpose: Fatty acid amide hydrolase (FAAH) is an intracellular serine amidase that terminates the signalling of various lipid messengers involved in pain regulation, including anandamide and palmitoylethanolamide. Here, we investigated the effects of pharmacological or genetic FAAH removal on tolerance to the antinociceptive effects of morphine.

Experimental Approach: We induced tolerance in male and female mice by administering twice-daily morphine for 7 days while monitoring nociceptive thresholds by the tail immersion test. The globally active FAAH inhibitor URB597 (1 and 3 $mg{\cdot}kg^{-1}$, i.p.) or the peripherally restricted FAAH inhibitor URB937 (3 $mg{\cdot}kg^{-1}$, i.p.) were administered daily 30 min prior to morphine, alone or in combination with the cannabinoid CB_1 receptor antagonist AM251 (3 $mg{\cdot}kg^{-1}$, i.p.), the CB_2 receptor antagonist AM630 (3 $mg{\cdot}kg^{-1}$, i.p.), or the PPAR-α antagonist GW6471 (4 $mg{\cdot}kg^{-1}$, i.p.). Spinal levels of FAAH-regulated lipids were quantified by LC/MS-MS. Gene transcription was assessed by RT-qPCR.

Key Results: URB597 prevented and reversed morphine tolerance in both male and female mice. This effect was mimicked by genetic FAAH deletion, but not by URB937. Treatment with AM630 suppressed, whereas treatment with AM251 or GW6471, attenuated the effects of URB597. Anandamide mobilization was enhanced in the spinal cord of morphine-tolerant mice. mRNA levels of the anandamide-producing enzyme *N*-acyl-phosphatidylethanolamine PLD (NAPE-PLD) and the palmitoylethanolamide receptor PPAR-α, but not those for CB_2 , CB_1 receptors or FAAH, were elevated in spinal cord

Conclusion and Implications: FAAH-regulated lipid signalling in the CNS modulated opiate tolerance, suggesting FAAH as a potential target for opiate-sparing medications.

1 | INTRODUCTION

Chronic pain affects more than 20% of American adults, and its management remains unsatisfactory (Dahlhamer et al., 2018). Despite contrasting clinical evidence, persistent painful conditions continue to be widely treated with opiate drugs (Choi, 2016; Fields, 2011). Indeed, in 2017 alone, more than 56 million Americans were prescribed an opiate analgesic, in many cases to treat chronic pain (Centers for Disease Control and Prevention, 2018). The pervasive overuse of prescription opiates is considered to be a major contributing factor in the

Abbreviations: AEA, arachidonoylethanolamide, anandamide; ASTM, American Standard Test Sieve Series; Ct, cycle threshold; DSM-5, Diagnostic and Statistical Manual of Mental Disorders, 5th edition; ESI, electrospray ionization; FAAH, fatty acid amide hydrolase; LOD, limit of detection; LOQ, limit of quantification; *m/z*, mass to charge ratio
NAPE-PLD, *N*-acylphosphatidylethanolamine PLD; NMDA, *N*-methyl-D-aspartate; OEA, oleoylethanolamide; OUD, opioid use disorders; PEA, palmitoylethanolamide; PEG400, polyethylene glycol 400; RT-qPCR, real-time polymerase chain reaction.

epidemic of opioid use disorder (OUD) and opiate-related overdose deaths that is currently gripping the United States (Volkow & Collins, 2017).

Tolerance to the analgesic effects of the opiates is one of the diagnostic criteria for OUD (DSM-5) and a major challenge in the clinical use of these drugs (American Psychiatric Association, 2013; Corder et al., 2017; Inturrisi, 2002). To overcome it, physicians tend to increase doses or switch to more potent opiates (Hayhurst & Durieux, 2016; Morgan & Christie, 2011), thus heightening the risk of OUD, overdosing, and diversion (Volkow & Collins, 2017). The molecular mechanisms underlying opiate tolerance are still only partially understood but are thought to require profound changes in the G-protein coupling of **μ-type opioid receptors** along with intracellular and transcellular compensatory processes in the peripheral system and CNS (Corder et al., 2017; Maduna et al., 2018). Untangling these interactions is complex but essential to uncover control points of opiate tolerance, which might be targeted by therapy.

Fatty acid amide hydrolase (**FAAH**), a member of the amidase family of enzymes (McKinney & Cravatt, 2005), catalyses the intracellular breakdown of several structurally and functionally distinct classes of bioactive fatty acyl amides, including endogenous agonists at G protein-coupled **cannabinoid receptors**, such as **anandamide** (Devane et al., 1992), at the nuclear **PPAR-α**, such as **oleoylethanolamide** (OEA) and **palmitoylethanolamide** (PEA) (Fu et al., 2003; LoVerme, La Rana, Russo, Calignano, & Piomelli, 2005), and at **TRPV1** channels, such as OEA (Ahern, 2003; LoVerme et al., 2006). Studies in animal models have shown that small molecules FAAH inhibitors attenuate pain-related behaviours (Russo et al., 2007; Woodhams, Chapman, Finn, Hohmann, & Neugebauer, 2017) and augment the antinociceptive actions of **morphine** (Slivicki et al., 2018; Wilkerson et al., 2017), pointing to FAAH as a potential therapeutic target for opiate-sparing medications.

These findings, along with the known functional links between the endogenous opioid and endocannabinoid signalling systems (Roques, Fournie-Zaluski, & Wurm, 2012), prompted us to examine whether FAAH blockade might influence the development of morphine tolerance. Using male and female mice, we found that central, but not peripheral, FAAH inhibition counters the induction and reverses established morphine tolerance through a mechanism that involves at least three distinct receptor systems—**CB_2** and **CB_1** receptors and PPAR-α—recruited by FAAH-regulated lipid signals.

What is already known

- Endocannabinoids and endogenous opioids cooperate in the control of pain processing.
- FAAH inhibitors augment the antinociceptive effects of opioids.

What this study adds

- Inhibition of FAAH activity in the CNS prevents and reverses tolerance to morphine-induced antinociception.

What is the clinical significance

- FAAH may provide a therapeutic target for the treatment of morphine tolerance.

2 | METHODS

2.1 | Animals

All animal care and experimental procedures complied with the Guide for the Care and Use of Laboratory Animals as promulgated by the U.S. National Institutes of Health and were approved by the Animal Care and use Committee of the University of California, Irvine. Animal studies are reported in compliance with the ARRIVE guidelines (Kilkenny, Browne, Cuthill, Emerson, & Altman, 2010) and with the recommendations made by the *British Journal of Pharmacology*.

We used male and female CD1 mice weighing 25–30 g (Harlan Laboratories, Indianapolis, USA) and FAAH-null ($FAAH^{-/-}$) mice (25–30 g), which had been backcrossed to C57BL/6J mice for more than 10 generations (Cravatt et al., 2001). The animals were randomly assigned to treatment groups and housed in standard ventilated clear plastic cages (three to five per cage) with conventional wood chips bedding in the animal facility of the University of California, Irvine. They were maintained in a pathogen free-environment on 12-hr light/dark cycle at controlled temperature (22°C) and humidity (50–60%). Food and water were available ad libitum. Before the start of the experiments, animals were handled for three consecutive days (about 3 min per animal per day), and behavioural testing was conducted during the light phase of the light/dark cycle. Efforts were made to minimize the number of animals used and their discomfort.

2.2 | Drug administration

Morphine sulfate was dissolved in distilled water and injected s.c. (15 and 30 $mg{\cdot}kg^{-1}$; 10 $ml{\cdot}kg^{-1}$) 45 min prior to testing. AM251 (3 $mg{\cdot}kg^{-1}$; Chambers, Koopmans, Pittman, & Sharkey, 2006), AM630 (3 $mg{\cdot}kg^{-1}$; Ibrahim et al., 2005), GW6471 (4 $mg{\cdot}kg^{-1}$; Donvito, Wilkerson, Damaj, & Lichtman, 2016), URB597 (1 and 3 $mg{\cdot}kg^{-1}$; Piomelli et al., 2006), and URB937 (3 $mg{\cdot}kg^{-1}$; Sasso et al., 2012) were dissolved in a mixture of PEG400:Tween80:distilled water (5:5:90, v/v/v; 10 $ml{\cdot}kg^{-1}$) and injected i.p.. AM251, AM630, and GW6471 were given 15 min prior to URB597 and URB937, which were given 30 min prior to morphine. Animals were immediately returned into their home cages after treatment.

2.3 | Behavioural testing

Tolerance to the antinociceptive effect of morphine was induced as described (Contet, Filliol, Matifas, & Kieffer, 2008; de Guglielmo

et al., 2014; Heinzen & Pollack, 2004; Mamiya et al., 2001). Morphine was administered twice daily at 9:00 and 17:00 for 7 days at the following doses: Day 1 = 15 mg·kg^{-1}; Days 2–6 = 30 mg·kg^{-1}; Day 7 = 15 mg·kg^{-1}. A reduced dose of morphine was used on Days 1 and 7 so that the effects of the drug before and after tolerance development could be directly compared. In some experiments, mice were treated with URB597 or URB937 (i.p.) 30 min prior to morphine. Nociceptive responses were monitored on alternate days using the tail immersion test, 30 min following the second morphine injection (17:00). The mice were restrained in a soft tissue pocket, the distal half of the tail was dipped into a water bath set at 54°C, and the withdrawal latency was measured. Cut-off time was set at 10 s. Two tail-withdrawal measures (separated by 30 s) were recorded and averaged. At the end of some experiments, the entire spinal cord was collected, after anaesthesia with isoflurane, as described earlier (Richner, Jager, Siupka, & Vaegter, 2017) for analyses. All data analyses were performed under blinded conditions.

2.4 | Lipid extractions

Anandamide, PEA, and OEA were extracted from frozen spinal cord tissue using a modified Bligh and Dyer method (Astarita & Piomelli, 2009). Frozen spinal cords were weighed and homogenized in methanol (1 ml) containing the following internal standards: [$^2H_4$]-anandamide (20 pmol), [$^2H_4$]-PEA (200 pmol), and [$^2H_4$]-oleoylethanolamide (OEA; 200 pmol). Chloroform (2 ml) was added, and the organic phases were washed with water (1 ml). The homogenized mixtures were centrifuged, and the organic phases were collected. After evaporating the solvent under N_2, residues were dissolved in chloroform (1 ml) and loaded onto small glass columns packed with Silica Gel G (60-Å 230-400 Mesh ASTM; Whatman, Clifton, NJ). Analytes were eluted with chloroform/methanol (9:1, 2 ml), dried under N_2, and reconstituted in chloroform/methanol (1:9, 80 μl) for LC/MS-MS analysis.

2.5 | LC/MS-MS analysis

We used a 1260 series binary pump LC system coupled to a 6460C triple quadrupole MS (Agilent Technologies, Inc., Santa Clara, CA) equipped with an electrospray ionization (ESI) interface. Analytes were separated using an XDB C18 column (50 × 2.1 mm i.d., 1.8-μm, Zorbax), eluted with a mobile phase consisting of solvent A (0.25% acetic acid and 5-mM ammonium acetate in water) and solvent B (0.25% acetic acid and 5-mM ammonium acetate in methanol) at a flow rate of 0.2 ml·min^{-1}. Column temperature was kept at 40°C. MS detection was in the positive electrospray mode, and the capillary voltage was set at 3.5 kV. N_2 was used as drying gas at a flow rate of 10 L·min^{-1} and a temperature of 300°C. Lipid were identified using the mass to charge (*m/z*) ratios of precursor and product ions and quantified by isotope dilution. The ion mass transitions used were as follows: anandamide (*m/z* 348.3/62.0), [$^2H_4$]-anandamide (*m/z* 352.3 > 62.0), PEA (*m/z* 300.3 > 62.0) and [$^2H_4$]-PEA (*m/z* 304.3 > 62.0), OEA (*m/z* 326.3 > 62.0), and [$^2H_4$]-OEA (*m/z* 330.3 > 62.0). Data analyses were performed using Agilent MassHunter Workstation Software Quantitative Analysis (Agilent MassHunter Quantitative Analysis software, RRID:SCR_015040). The limit of detection (LOD) and the limit of quantification (LOQ) were anandamide (LOD = 2.5 fmol·ml^{-1}; LOQ = 5 fmol·ml^{-1}), PEA (LOD = 5 fmol·ml^{-1}; LOQ = 10 fmol·ml^{-1}), and OEA (LOD = 5 fmol·ml^{-1}; LOQ = 10 fmol·ml^{-1}).

2.6 | Molecular studies

Frozen spinal cords were homogenized in 2-ml ice-cold TRIzol™ reagent (Invitrogen Life Technologies, Carlsbad, CA) according to supplier's instructions. DNAse was added to samples for total RNA clean-up using the PureLink RNA mini-kit (Invitrogen Life Technologies). RNA concentration and purity were determined using a SpectraMax M5 spectrophotometer (Molecular Devices, LLC., San Jose, CA, USA). For cDNA synthesis, 2 μg of purified RNA was reverse transcribed using superscript VILO cDNA synthesis kit in a total volume of 20 μl for 2 hr at 45°C according to the manufacturer's instruction (Invitrogen Life Technologies), and the final concentration of cDNA was 100 ng·μl^{-1}. First-strand cDNA was amplified using the iQ SYBR Green Super Mix (Invitrogen Life Technologies). Primer sequences for the targeted genes were as follows *Faah*: 5′-GCCTCAAGG AATGCTTCAGC- 3′ (forward) and 5′-TGCCCTCATTCAGGCTCAAG-3′ (reverse); *Napepld*: 5′-CAGCGGCGTTCCAGGTTCC-3′ (forward) and 5′-GCTCCGATGGGAATGGCCGC-3′ (reverse); *Ppara*: 5′-AGCT GGTGTAGCAAGTGT-3′ (forward) and 5′-TCTGCTTTCAGTTTT GCTTT-3′ (reverse); *Cnr$_1$*: 5′-TGAAGTCGATCTTAGACGGCC-3′ (forward) and 5′-GTGGTGATGGTACGGAAGGTA-3′ (reverse) and *Cnr$_2$*: 5′-CAGGACAGGCTTCACAAGAC-3′ (forward) and 5′-GACAGGC TTTGGCTGCTTCTAC-3′ (reverse). Quantitative PCR was performed in a 96-well PCR plate and run at 95°C for 10 min, followed by 40 cycles, each consisting of 15 s at 95°C and 1 min at 60°C, using Stratagene Mx3000P (Stratagene Mx3000P™ qPCR system, Agilent). Two publicly available software programs NormFinder (NormFinder, RRID:SCR_003387) and BestKeeper (BestKeeper, RRID:SCR_003380) were used to determine the expression stability and the geometric mean of three different housekeeping genes (*Gapdh*, *Actb*, and *Hprt*). Δ*Ct* values were calculated by subtracting the *Ct* value of the geometric mean of these housekeeping genes from the *Ct* value for the gene of interest. The relative quantity of genes of interest was calculated by the expression, $2^{-\Delta\Delta Ct}$.

2.7 | Data and statistical analysis

The data and statistical analysis comply with the recommendations of the *British Journal of Pharmacology* on experimental design and analysis in pharmacology (Curtis et al., 2018). All the data were analysed by Levene's test and met the assumption of homogeneity of variances (P > .1). The effect of URB597 on the development and established

morphine tolerance was analysed separately in male and female by two-way repeated measures ANOVA with treatment as the between-subject factor and time (days) as the within-subject factor. The effects of URB597, URB937, AM251, AM630, GW6471, or their combinations were analysed by two-way repeated measures ANOVA with treatments as the between-subject factor and time (days) as the within-subject factor. Differences in the development of morphine tolerance in $FAAH^{-/-}$ mice and wild-type (WT) controls were assessed by mixed-factorial ANOVA with strains ($FAAH^{-/-}$ and WT) and treatment (morphine or distilled water) as the between-subject factors and time (days) as the within-subject factor. Changes in lipid amides and gene expression levels were compared using unpaired Student's *t* test and one-way ANOVA. Where appropriate, a Bonferroni's multiple comparison test was performed. Statistical significance was set at $^{*}P < .05$. Analyses were performed with either GraphPad Prism version 6.0 (GraphPad Prism, RRID:SCR_002798) or the Statistical Package for Social Science program SPSS® (SPSS, RRID: SCR_002865). No data were transformed or excluded.

2.8 | Chemicals

Morphine sulfate, AM251, AM630, and GW6471 were purchased from Sigma-Aldrich (St. Louis, MO, USA). URB597 and URB937 were synthesized at Pharmaron (Tianjin, China) using published synthetic methods (Mor et al., 2004; Moreno-Sanz et al., 2013). Purity was >99%, as assessed by LC/MS-MS (Vozella et al., 2019). [$^2H_4$]-anandamide, [$^2H_4$]-PEA, and [$^2H_4$]-OEA were obtained from Tocris (Minneapolis, MN, USA).

2.9 | Nomenclature of Targets and Ligands

Key protein targets and ligands in this article are hyperlinked to corresponding entities in http://www.guidetopharmacology.org, the common portal for data from the IUPHAR/BPS Guide to PHARMACOLOGY (Harding et al., 2018), and are permanently archived in the Concise Guide to PHARMACOLOGY 2019/20 (Alexander, Christopoulos, et al., 2019; Alexander, Cidlowski et al., 2019; Alexander, Fabbro, et al., 2019; Alexander, Mathie et al., 2019).

3 | RESULTS

3.1 | Effects of global FAAH inhibition on the induction of morphine tolerance

To investigate the effects of FAAH blockade on the development of morphine tolerance, we treated six groups of male CD1 mice (n = 8 per group) with morphine (15 or 30 mg·kg^{-1}, s.c., see Section 2), the globally active FAAH inhibitor URB597 (1 and 3 mg·kg^{-1}, i.p.), a combination of the two (URB597 given 30 min prior to morphine), or their respective vehicles. Previous work has shown that the doses of URB597 selected for this experiment fully inhibit FAAH activity and enhance anandamide-mediated signalling in mouse brain (Fegley et al., 2005; Wei et al., 2015). As illustrated in Figure 1, morphine produced significant antinociception on Test Days 1 and 3. This effect progressively decreased on the following days, when it became statistically undetectable. At both the 1 and 3 mg·kg^{-1} doses, URB597 prevented the development of morphine tolerance without altering nociceptive thresholds (Figure 1a,b).

To determine whether sexual dimorphisms might exist in the response to URB597, we repeated the experiments in four groups of female CD1 mice (n = 8 per group). Statistical analyses revealed a significant antinociceptive effect of morphine from Test Days 1 to 5, which disappeared on the following days (Figure 1c). As observed in male mice (Figure 1a), co-administration of URB597 (3 mg·kg^{-1}, i.p.) prevented the induction of morphine tolerance in female mice without changing nociceptive thresholds (Figure 1c,d).

3.2 | Effects of global FAAH deletion on the induction of morphine tolerance

To further test the role of FAAH in morphine tolerance, we treated two groups of $FAAH^{-/-}$ mice and two groups of WT C57BL6/J mice (n = 7 per group), both male, with morphine or saline. Statistical analyses demonstrated a significant antinociceptive effect of morphine in both mouse lines on Test Days 1 and 3 (Figure 2a). The effect tapered off in WT animals on Days 5 and 7, but strikingly persisted in $FAAH^{-/-}$ animals (Figure 2a,b). FAAH deletion did not change baseline nociceptive responding in the absence of morphine (Figure 2a,b).

3.3 | Effects of peripheral FAAH inhibition on the induction of morphine tolerance

To assess whether URB597 attenuates morphine tolerance by inhibiting central or peripheral FAAH activity, we treated four groups of mice (n = 7–8 per group) with morphine alone or in combination with the peripherally restricted FAAH inhibitor URB937. The compound was administered 30 min prior to morphine at a dose (3 mg·kg^{-1}, i.p.) that is known to inhibit FAAH activity exclusively outside the brain and spinal cord (Clapper et al., 2010; Moreno-Sanz et al., 2013). Significant morphine tolerance was observed on Test Days 5 and 7, irrespective of whether the mice were treated with the opiate alone or in combination with URB937 (Figure 3a,b). URB937 did not affect nociceptive responding when administered alone (Figure 3a).

3.4 | Effects of global FAAH inhibition on established morphine tolerance

We also evaluated whether FAAH inhibition might reverse established tolerance to morphine antinociception. Three groups of male mice

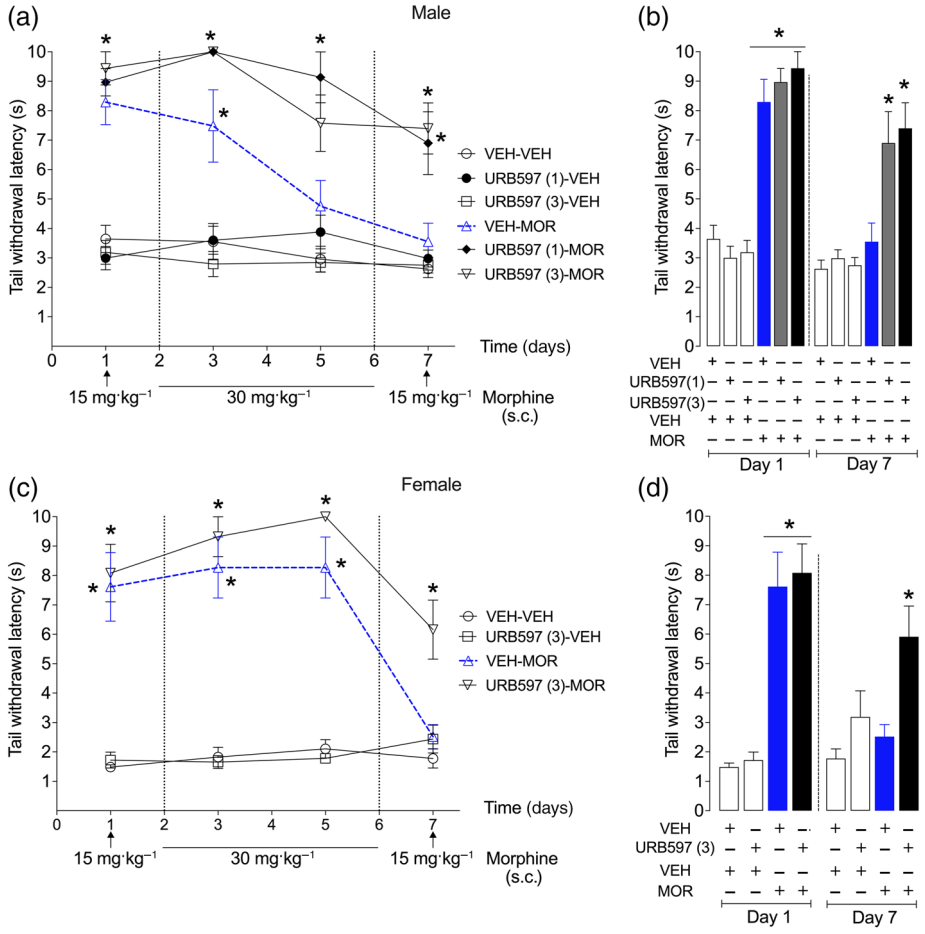

FIGURE 1 Effects of the global FAAH inhibitor URB597 on the development of morphine tolerance. Male and female mice were treated daily with vehicle, URB597 ((1) and (3) mg·kg^{-1}, i.p., 30 min prior to morphine), morphine (15 or 30 mg·kg^{-1}, s.c.), or their combination. Nociceptive thresholds were measured on alternate days using the tail immersion test. (a [male], c [female]) Time course of the effects of the global FAAH inhibitor URB597, morphine, and their combination. (b [male], d [female]) Changes in nociceptive thresholds on Test Days 1 (right) and 7 (left). Results shown are the means ± SEM (n = 8 per group). *P < .05, significantly different from vehicle-treated animals

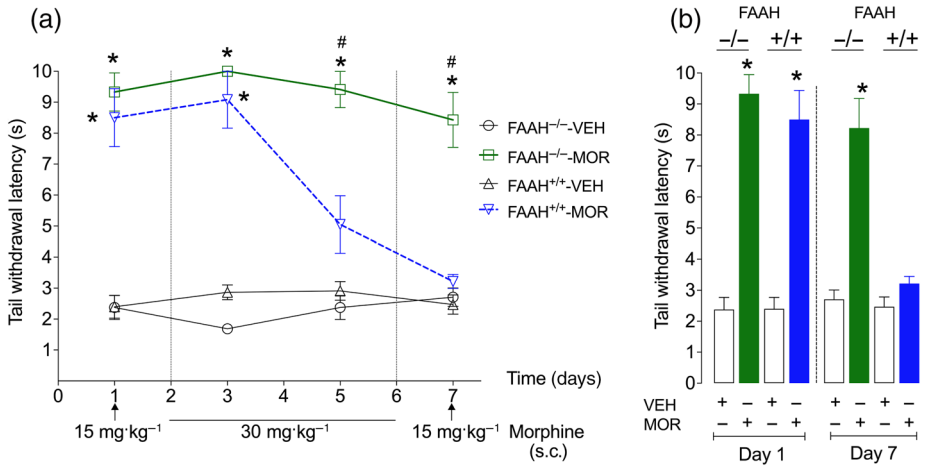

FIGURE 2 Effects of genetic FAAH deletion on the development of morphine tolerance. FAAH−/− and wild type (WT) mice were divided into four groups and treated with morphine (15 or 30 mg·kg^{-1}, s.c.) or vehicle. (a) Time course of the effects of morphine or vehicle. (b) Changes in nociceptive thresholds on Test Days 1 (right) and 7 (left). Results shown are the means ± SEM (n = 7 per group). *P < .05, significantly different from vehicle-treated mice. #P < .05, significantly different from WT mice

and two groups of female mice (n = 8 per group) were treated twice daily with vehicle or morphine (15 or 30 mg·kg^{-1}, s.c.; see Section 2). Upon repeated exposure, the antinociceptive effects of morphine disappeared (Test Day 7, Figure 4) but was reinstated on Day 8 following a single administration of URB597 (1 or 3 mg·kg^{-1}, i.p.) in both male (Figure 4a) and female (Figure 4b) animals.

3.5 | Effect of morphine tolerance on gene transcription

Next, we asked whether morphine tolerance might be accompanied by transcriptional changes in genes implicated in the metabolism and function of anandamide and other fatty acid ethanolamides

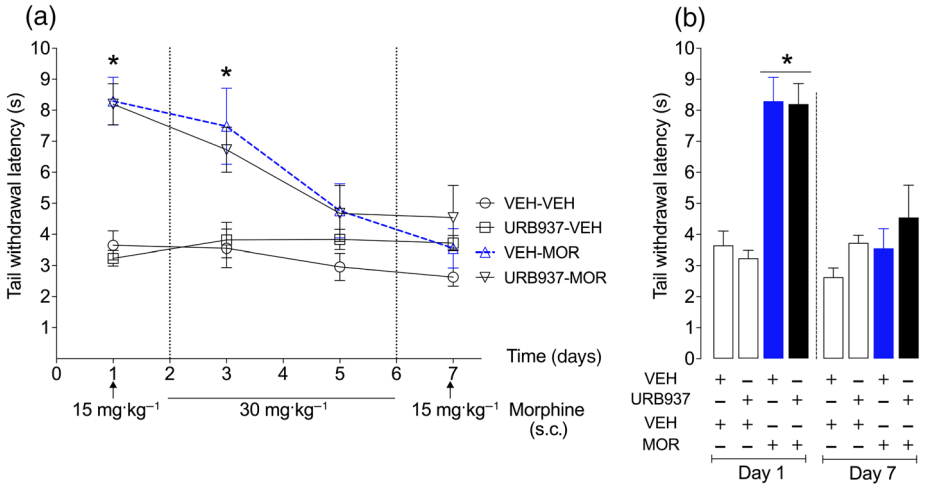

FIGURE 3 Effects of the peripheral FAAH inhibitor URB937 on the development of morphine tolerance. (a) Time course of the effects of the peripheral FAAH inhibitor URB937 (3 mg·kg^{-1}, i.p.), morphine, and their combination in the tail immersion test. (b) Changes in nociceptive thresholds on Test Days 1 (right) and 7 (left). Results shown are the means ± SEM (n = 8 per group). *P < .05, significantly different from vehicle-treated animals

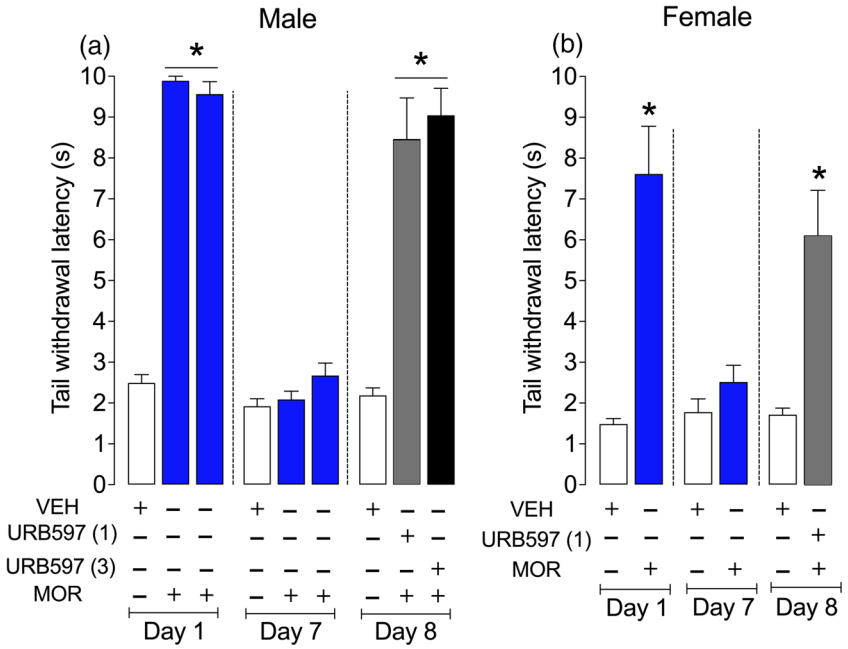

FIGURE 4 Effects of the global FAAH inhibitor URB597 on established morphine tolerance. Male (a) and female (b) mice were treated daily with morphine or vehicle. Nociceptive thresholds were measured using the tail immersion test in the absence (Days 1 [right] and 7 [centre]) and presence (Day 8 [left]) of URB597 ((1) and (3) mg·kg^{-1}, i.p.). Results shown are the means ± SEM (n = 8 per group). *P < .05, significantly different from versus vehicle-treated animals

(Piomelli & Sasso, 2014). In addition to FAAH (encoded in mice by the *Faah* gene), we measured mRNA levels of *Napepld*, which encodes for the FAE-producing enzyme *N*-acylphosphatidylethanolamine PLD (NAPE-PLD; Kaczocha, Glaser, Chae, Brown, & Deutsch, 2010; Maccarrone, 2017; Tsuboi, Uyama, Okamoto, & Ueda, 2018; Ueda, Tsuboi, & Uyama, 2013) and genes encoding for CB_1 (*Cnr*$_1$), CB_2 (*Cnr*$_2$), and PPAR-α (*Ppara*). Two groups of mice (n = 7–8 per group) were rendered tolerant to morphine (Figure 5a). The entire spinal cords of five mice from each of these groups were collected, and RNA extracts were subjected to RT-qPCR analysis. As shown in Figure 5b, mRNA levels of *Napepld* and *Ppara* were significantly elevated in morphine-tolerant mice relative to vehicle-treated controls. By contrast, no significant changes were observed in the levels of *Faah*, *Cnr*$_1$, or *Cnr*$_2$ (Figure 5b).

3.6 | Effect of morphine tolerance on levels of fatty acid ethanolamides in spinal cord

The observed increase in NAPE-PLD transcription (Figure 6b) suggests that morphine tolerance might be accompanied by enhanced production of fatty acid ethanolamides in the spinal cord. To investigate this possibility, we measured fatty acid ethanolamide content in morphine-tolerant mice treated with URB597 or its vehicle. We found that the levels of anandamide (Figure 6a), PEA (Figure 6b), and OEA (Figure 6c) were unchanged in morphine-tolerant mice, compared to mice treated only with URB597 (3 mg·kg^{-1}, i.p.). Notably, however, one-way ANOVA revealed an increase in anandamide content in spinal cord of mice treated with both morphine and URB597 (Figure 6a). No such effect was observed for PEA (Figure 6b) or OEA

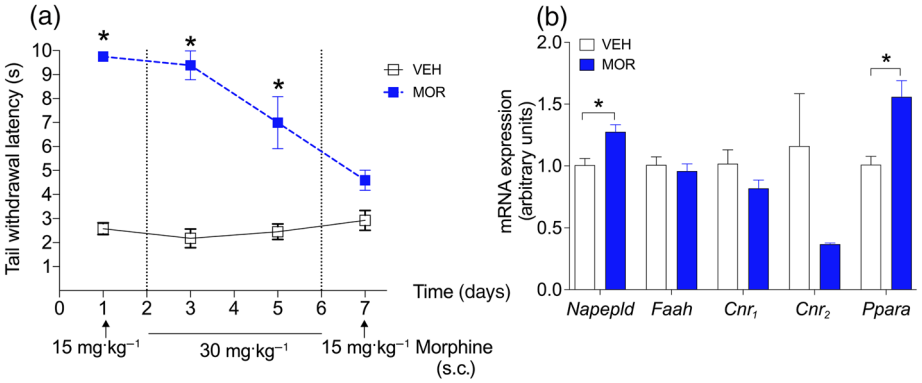

FIGURE 5 Levels of mRNA from genes related to fatty acid ethanolamides in morphine-tolerant mice. (a) Time course of the development of morphine tolerance in CD1 mice. (b) Transcriptional changes in Napepld, Faah, Ppara, Cnr1, and Cnr2 were evaluated in the spinal cord of the mice shown in (a). Results shown are the means ± SEM (n = 5 per group). *P < .05, significantly different from vehicle-treated animals

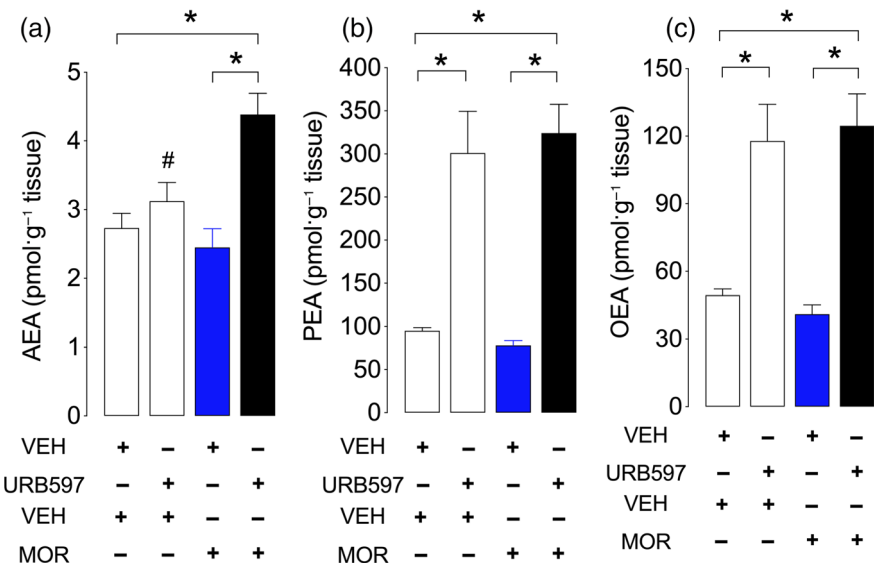

FIGURE 6 Levels of fatty acid ethanolamides in spinal cord of morphine-tolerant mice. Spinal cord levels of anandamide (a), PEA (b), and OEA (c) in morphine-tolerant mice treated with URB597 (3 mg·kg^{-1}, i.p.) or vehicle. Results shown are the means ± SEM (n = 5 per group). *P < .05, significantly different from vehicle-treated animals. #P < .05, significantly different from URB597-treated mice

(Figure 6c). The results suggest that morphine tolerance may be associated with accelerated anandamide mobilization (i.e., increased production and/or reduced degradation), which is unmasked by FAAH inhibition.

3.7 | Effects of antagonists of CB_1 receptors or PPAR-α

We asked whether activation of CB_1 receptors or PPAR-α, by FAAH-regulated lipid messengers might contribute to the effects of URB597. We treated eight groups of mice (n = 7 per group) with morphine, URB597 (3 mg·kg^{-1}, i.p.), AM251 (3 mg·kg^{-1}, i.p.), their combination (AM251 was given 15 min before URB597), or the respective vehicles. AM251 is a highly potent CB_1 receptor antagonist/inverse agonist (IC_{50} = 8 nM; Lan et al., 1999), and the dose selected for this experiment fully counters the CB_1-mediated effects of URB597 in mice and rats (Danandeh et al., 2018; Fegley et al., 2005; Wei et al., 2015). As previously shown, co-administration of URB597 prevented the development of morphine tolerance (Figure 7a,b). This effect was attenuated but not completely reversed by AM251 (Figure 7a,b), which per se did not influence nociceptive responding or tolerance induction (Figure 7a).

In a subsequent experiment, we treated eight groups of mice (n = 7 per group) with morphine, URB597 (3 mg·kg^{-1}, i.p.), GW6471 (4 mg·kg^{-1}, i.p.), their combination (GW6471 was given 15 min before URB597) or their respective vehicles. The PPAR-α antagonist GW6471 (IC_{50} = 0.24 μM; Xu et al., 2002) was previously shown to block PPAR-α-mediated responses at doses of 2 mg·kg^{-1} or greater (Donvito et al., 2016). GW6471 caused a significant decrease in the nociceptive response to morphine on Test Day 3 (Figure 8a). Additionally, as seen with CB_1 receptor blockade, GW6471 partly reinstated morphine tolerance in the presence of URB597 (Figure 8a,b) without influencing nociceptive thresholds when administered alone or in combination with the FAAH inhibitor (Figure 8a).

3.8 | Effect of CB_2 receptor antagonist

Finally, we asked whether the effects of URB597 might involve CB_2 receptor activation. We treated eight groups of mice (n = 8 per group)

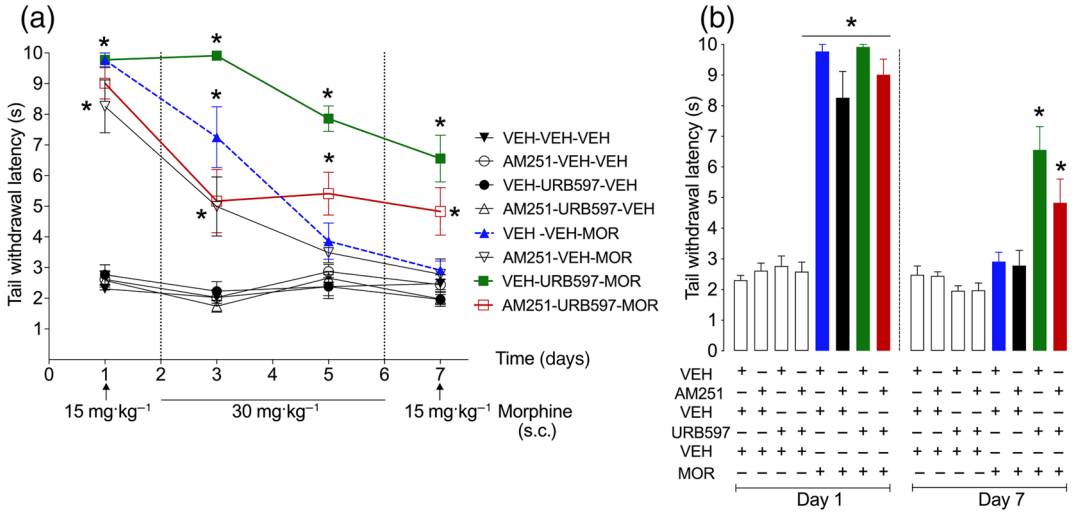

FIGURE 7 Effects of the CB_1 receptor antagonist AM251. (a) Time course of the effects of URB597 (3 mg·kg^{-1}, i.p.), AM251 (3 mg·kg^{-1}, i.p.), morphine, and their combination in the tail immersion test. (b) Changes in nociceptive thresholds on Test Days 1 (right) and 7 (left). Results shown are the means ± SEM (n = 8 per group). *P < .05, significantly different from vehicle-treated animals

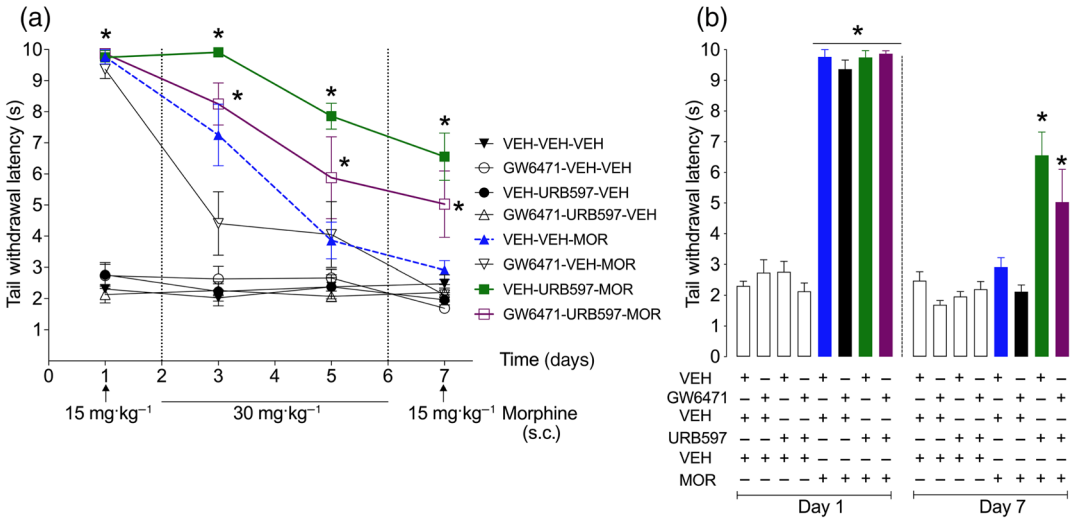

FIGURE 8 Effects of the PPAR-α antagonist GW6471. (a) Time course of the effects of URB597 (3 mg·kg^{-1}, i.p.), GW6471 (4 mg·kg^{-1}, i.p.), morphine, and their combination in the tail immersion test. (b) Changes in nociceptive thresholds on Test Days 1 (right) and 7 (left). Results shown are the means ± SEM (n = 8 per group). *P < .05, significantly different from vehicle-treated animals

with morphine, URB597 (3 mg·kg^{-1}, i.p.), AM630 (3 mg·kg^{-1}, i.p.), their combination (AM630 was given 15 min before URB597), or the respective vehicles. AM630 is a highly potent CB_2 receptor antagonist/inverse agonist (IC_{50} = 1.9 μM) and has 70- to 165-fold selectivity for CB_2 over CB_1 receptors (Hosohata et al., 1997). The dose of AM630 selected for this experiment fully antagonizes CB_2 receptor-mediated responses in mice (Ibrahim et al., 2005). AM630 did not per se alter the antinociceptive trajectory of morphine (Figure 9a) but completely blocked the effects of URB597 (Figure 9a, b). AM630 did not change nociceptive responding when administered alone or in combination with URB597 (Figure 9a,b).

4 | DISCUSSION

The main finding of the present study is that the CNS-penetrant FAAH inhibitor URB597 prevented and reversed tolerance to the antinociceptive effects of morphine in mice of both sexes. This effect is reproduced by genetic FAAH deletion but not by administration of the peripherally restricted FAAH inhibitor URB937. We interpret these findings as suggesting that FAAH-regulated lipid messengers, such as anandamide or PEA, counter morphine tolerance via a centrally mediated mechanism. In addition, we found that selective antagonists of CB_2 or CB_1 receptors, and of PPAR-α fully suppress (CB_2) or

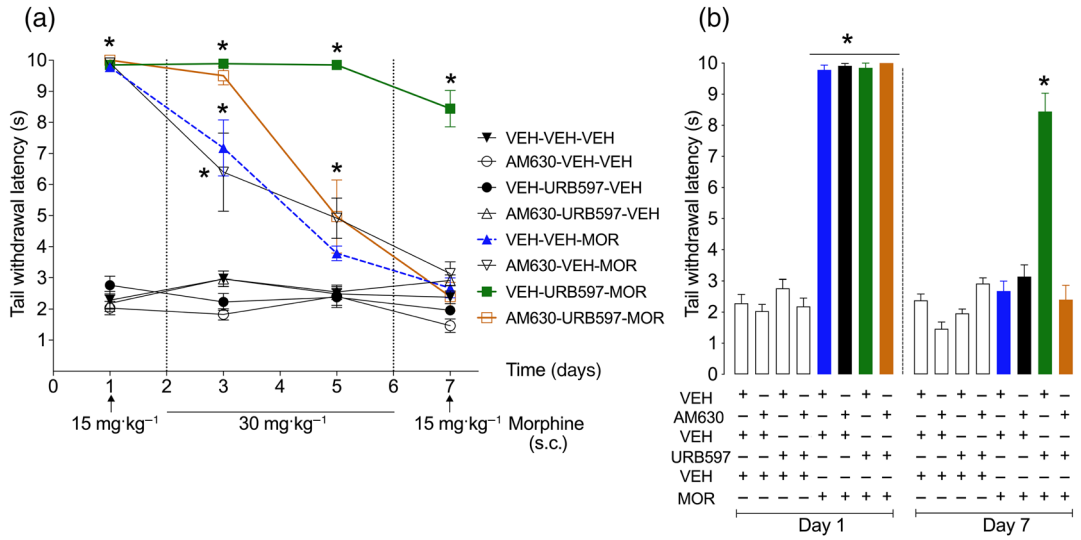

FIGURE 9 Effects of the CB_2 receptor antagonist AM630. (a) Time course of the effects of URB597 (3 mg·kg^{-1}, i.p.), AM630 (3 mg·kg^{-1}, i.p.), morphine, and their combination in the tail immersion test. (b) Changes in nociceptive thresholds on Test Days 1 (right) and 7 (left). Results shown are the means ± SEM (n = 8 per group). *P < .05, significantly different from vehicle-treated animals

attenuate (CB_1 and PPAR-α) the effects of URB597. Of note, the development of morphine tolerance was accompanied by enhanced mobilization of anandamide and heightened transcription of NAPE-PLD, a membrane-associated phospholipase involved in the formation of anandamide and other FAEs (Hussain, Uyama, Tsuboi, & Ueda, 2017; Magotti et al., 2015), in spinal cord tissue. The results support a role for central FAAH-regulated lipid signalling in the modulation of opiate tolerance and identify FAAH as a potential target for opiate-sparing medications.

Intracellular FAAH activity controls the availability of several structurally and functionally distinct classes of lipid-derived messengers. These include endogenous agonists at G protein-coupled cannabinoid receptors (anandamide; Devane et al., 1992), nuclear PPAR-α receptors (OEA and PEA; Fu et al., 2003; LoVerme et al., 2005), TRPV1 channels (OEA; LoVerme et al., 2006) and unidentified receptor(s) involved in skin wound healing (*N*-acyl-taurines; Sasso et al., 2016). This multiplicity of physiological functions is reflected in the rich pharmacology of FAAH inhibitors. While many of the effects exerted by these agents—including reduced anxiety-, depression-, and pain-related behaviours in animal models (Bortolato et al., 2007; Gobbi et al., 2005; Russo et al., 2007)—may primarily depend on increased anandamide activity at cannabinoid receptors, other responses appear to involve the amplification of different FAAH-regulated lipid signals. For example, endogenous PPAR-α agonists (most likely PEA and/or OEA) have been implicated in the effects of FAAH inhibition on acute nausea (Rock et al., 2017), cognition (Mazzola et al., 2009; Panlilio et al., 2016), and inflammatory pain (Sagar, Kendall, & Chapman, 2008). Synergistic interactions between CB_1 receptors and PPAR-α have also been documented (Calignano, La Rana, Giuffrida, & Piomelli, 1998; Russo et al., 2007). The results of our antagonist studies—reported in Figures 7, 8, and 9—suggest that FAAH inhibition prevents morphine tolerance by concomitantly enhancing anandamide-mediated activation of CB_1 and CB_2 receptors, along with PEA/OEA-mediated activation of PPAR-α. A possible mechanism underlying this interaction may be deduced from the experiments illustrated in Figures 5 and 6, which show that the development of morphine tolerance is accompanied by elevated NAPE-PLD transcription and accrued anandamide mobilization in spinal cord tissue. The latter effect is statistically detectable only when FAAH activity is blocked, however, likely owing to the high levels of such activity in the cord. Higher levels of anandamide is paralleled by enhanced transcription of PPAR-α (Figure 5), whose activation mediates the analgesic effects of PEA (LoVerme et al., 2005). While accounting for the available data, this scheme remains hypothetical. Further experiments are necessary to fill important knowledge gaps such as the cellular source and time course of anandamide formation, the localization of the receptors involved, and the possible participation of other FAAH-regulated lipid messengers. For example, FAAH also deactivates TRPV1 channel agonists such as OEA (Ahern, 2003; LoVerme et al., 2006), which appears to be involved in the potentiation of morphine tolerance (Chen, Geis, & Sommer, 2008). Indeed, pharmacological or genetic blockade of TRPV1 channel activity enhances morphine analgesia (Chen & Pan, 2006; Niiyama, Kawamata, Yamamoto, Furuse, & Namiki, 2009) and counters the development of morphine tolerance in animal models (Nguyen, Nam, Lee, Kim, & Jang, 2010). This suggests that the effect of FAAH inhibition on morphine tolerance could be partly masked by OEA-mediated activation of TRPV1 channels. Testing this possibility will require additional experimentation.

The development of tolerance to the analgesic effects of opiates sets a hard limit to the therapeutic usefulness of this important class of drugs and heightens the risk of misuse, dependence, and overdose-related deaths (Volkow & Collins, 2017). Current clinical strategies aimed at mitigating tolerance include opiate rotation (Smith & Peppin, 2014), concomitant administration of **NMDA receptor** antagonists such as **ketamine** (Assouline, Tramer, Kreienbuhl, & Elia, 2016)

or α_2-adrenoreceptor agonists such as clonidine (Tonner, 2017), and multimodal analgesia (Wick, Grant, & Wu, 2017). In the latter approach, pharmacological agents drawn from mechanistically distinct classes are combined to achieve greater-than-additive (i.e., synergistic) analgesic effects (Wick et al., 2017). For example, synergistic interactions between opiates and non-steroidal anti-inflammatory drugs have been successfully exploited to achieve greater control of post-operative pain (Campbell et al., 2019; Derry, Derry, & Moore, 2013). Recent experiments indicate that FAAH inhibitors synergize with morphine to attenuate pain-related responses (Slivicki et al., 2018; Wilkerson et al., 2017). Confirming and extending an earlier report (Hasanein & Ghafari-Vahed, 2016), the results presented here show that FAAH blockade counters the induction of morphine tolerance. This opioid-sparing effect appears to be mediated by a central mechanism that requires, unlike CB_1 receptor-mediated analgesia (Nozaki, Markert, & Zimmer, 2015; Russo et al., 2007), activation of at least three distinct receptor systems—CB_2, CB_1, and PPAR-α. Thus, a clinically relevant consequence of these findings is that combining an opiate analgesic with a CNS-penetrant FAAH inhibitor might offer an approach to multimodal analgesia that uniquely combines a synergistic interaction on pain control with an antagonistic interaction on tolerance development.

In conclusion, FAAH-regulated lipid signals such as anandamide and PEA are known to play a crucial role in the peripheral and central control of pain processing (Artukoglu, Beyer, Zuloff-Shani, Brener, & Bloch, 2017; Piomelli, Hohmann, Seybold, & Hammock, 2014; Piomelli & Sasso, 2014; Woodhams et al., 2017). The present results document a novel function for these messengers in the modulation of opiate tolerance and suggest FAAH inhibition as a potential therapeutic approach to the treatment of this condition.

ACKNOWLEDGEMENTS

This work was supported by NIH grants R42DA033683 and R41DA041871-01 (to D.P.).

AUTHOR CONTRIBUTIONS

Y.F. conducted behavioural testing and data analyses. F.P. performed the RT-qPCR. P.G.T. and F.A. ran lipid analyses. Y.F. and D.P. ideated the project and wrote the manuscript. All authors reviewed the final text version.

CONFLICT OF INTEREST

D.P. is an inventor in patent applications owned by the University of California, which describe systemic and peripheral FAAH inhibitors. Other authors have no conflict of interest.

DECLARATION OF TRANSPARENCY AND SCIENTIFIC RIGOUR

This Declaration acknowledges that this paper adheres to the principles for transparent reporting and scientific rigour of preclinical research as stated in the *BJP* guidelines for Design & Analysis and Animal Experimentation, and as recommended by funding agencies, publishers and other organisations engaged with supporting research.

REFERENCES

Ahern, G. P. (2003). Activation of TRPV1 by the satiety factor oleoylethanolamide. *The Journal of Biological Chemistry*, *278*, 30429–30434.

Alexander, S. P. H., Christopoulos, A., Davenport, A. P., Kelly, E., Mathie, A., Peters, J. A., … CGTP Collaborators. (2019). The concise guide to pharmacology 2019/20: G protein-coupled receptors. *British Journal of Pharmacology*, *176*, S21–S141.

Alexander, S. P. H., Cidlowski, J. A., Kelly, E., Mathie, A., Peters, J. A., Veale, E. L., … CGTP Collaborators. (2019). The concise guide to pharmacology 2019/20: Nuclear hormone receptors. *British Journal of Pharmacology*, *176*, S229–S246.

Alexander, S. P. H., Fabbro, D., Kelly, E., Mathie, A., Peters, J. A., Veale, E. L., … CGTP Collaborators. (2019). The concise guide to pharmacology 2019/20: Enzymes. *British Journal of Pharmacology*, *176*, S297–S396.

Alexander, S. P. H., Mathie, A., Peters, J. A., Veale, E. L., Striessnig, J., Kelly, E., … Collaborators, C. G. T. P. (2019). THE CONCISE GUIDE TO PHARMACOLOGY 2019/20: Ion channels. *British Journal of Pharmacology*, *176*, S142–S228. https://doi.org/10.1111/bph.14749

American Psychiatric Association. (2013). *Diagnostic and statistical manual of mental disorders* (Fifth ed.) (p. 541). Arlington, VA: American Psychiatric Association Press.

Artukoglu, B. B., Beyer, C., Zuloff-Shani, A., Brener, E., & Bloch, M. H. (2017). Efficacy of palmitoylethanolamide for pain: A meta-analysis. *Pain Physician*, *20*, 353–362.

Assouline, B., Tramer, M. R., Kreienbuhl, L., & Elia, N. (2016). Benefit and harm of adding ketamine to an opioid in a patient-controlled analgesia device for the control of postoperative pain: Systematic review and meta-analyses of randomized controlled trials with trial sequential analyses. *Pain*, *157*, 2854–2864.

Astarita, G., & Piomelli, D. (2009). Lipidomic analysis of endocannabinoid metabolism in biological samples. *Journal of Chromatography. B, Analytical Technologies in the Biomedical and Life Sciences*, *877*, 2755–2767.

Bortolato, M., Mangieri, R. A., Fu, J., Kim, J. H., Arguello, O., Duranti, A., … Piomelli, D. (2007). Antidepressant-like activity of the fatty acid amide hydrolase inhibitor URB597 in a rat model of chronic mild stress. *Biological Psychiatry*, *62*, 1103–1110.

Calignano, A., La Rana, G., Giuffrida, A., & Piomelli, D. (1998). Control of pain initiation by endogenous cannabinoids. *Nature*, *394*, 277–281.

Campbell, H. T., Yuhan, B. T., Smith, B., Misch, E., Svider, P. F., Pashkova, A. A., … Johnson, A. P. (2019). Perioperative analgesia for patients undergoing otologic surgery: An evidence-based review. *Laryngoscope*, *130*(1), 190–199.

Centers for Disease Control and Prevention. (2018). Annual surveillance report of drug-related risks and outcomes—United States, *Department of Health and Human Services*. August 31, 2018. Accessed from https://www.cdc.gov/drugoverdose/pdf/pubs/2018-cdc-drug-surveillance-report.pdf

Chambers, A. P., Koopmans, H. S., Pittman, Q. J., & Sharkey, K. A. (2006). AM 251 produces sustained reductions in food intake and body weight that are resistant to tolerance and conditioned taste aversion. *British Journal of Pharmacology*, *147*, 109–116.

Chen, S. R., & Pan, H. L. (2006). Loss of TRPV1-expressing sensory neurons reduces spinal μ opioid receptors but paradoxically potentiates opioid analgesia. *Journal of Neurophysiology*, *95*, 3086–3096.

Chen, Y., Geis, C., & Sommer, C. (2008). Activation of TRPV1 contributes to morphine tolerance: Involvement of the mitogen-activated protein kinase signaling pathway. *The Journal of Neuroscience*, *28*, 5836–5845.

Choi, C. Y. (2016). Chronic pain and opiate management. *Disease-a-Month*, *62*, 334–345.

Clapper, J. R., Moreno-Sanz, G., Russo, R., Guijarro, A., Vacondio, F., Duranti, A., … Piomelli, D. (2010). Anandamide suppresses pain initiation through a peripheral endocannabinoid mechanism. *Nature Neuroscience*, *13*, 1265–1270.

Contet, C., Filliol, D., Matifas, A., & Kieffer, B. L. (2008). Morphine-induced analgesic tolerance, locomotor sensitization and physical dependence do not require modification of μ opioid receptor, cdk5 and adenylate cyclase activity. *Neuropharmacology*, *54*, 475–486.

Corder, G., Tawfik, V. L., Wang, D., Sypek, E. I., Low, S. A., Dickinson, J. R., … Scherrer, G. (2017). Loss of μ opioid receptor signaling in nociceptors, but not microglia, abrogates morphine tolerance without disrupting analgesia. *Nature Medicine*, *23*, 164–173.

Cravatt, B. F., Demarest, K., Patricelli, M. P., Bracey, M. H., Giang, D. K., Martin, B. R., & Lichtman, A. H. (2001). Supersensitivity to anandamide and enhanced endogenous cannabinoid signaling in mice lacking fatty acid amide hydrolase. *Proceedings of the National Academy of Sciences of the United States of America*, *98*, 9371–9376.

Curtis, M. J., Alexander, S., Cirino, G., Docherty, J. R., George, C. H., Giembycz, M. A., … Ahluwalia, A. (2018). Experimental design and analysis and their reporting II: updated and simplified guidance for authors and peer reviewers. *British Journal of Pharmacology*, *175*, 987–993. https://doi.org/10.1111/bph.14153

Dahlhamer, J., Lucas, J., Zelaya, C., Nahin, R., Mackey, S., DeBar, L., … Helmick, C. (2018). Prevalence of chronic pain and high-impact chronic pain among adults—United States, 2016. *MMWR. Morbidity and Mortality Weekly Report*, *67*, 1001–1006.

Danandeh, A., Vozella, V., Lim, J., Oveisi, F., Ramirez, G. L., Mears, D., … Piomelli, D. (2018). Effects of fatty acid amide hydrolase inhibitor URB597 in a rat model of trauma-induced long-term anxiety. *Psychopharmacology*, *235*, 3211–3221.

Derry, S., Derry, C. J., & Moore, R. A. (2013). Single dose oral ibuprofen plus oxycodone for acute postoperative pain in adults. *Cochrane Database of Systematic Reviews*, (6), CD010289.

Devane, W. A., Hanus, L., Breuer, A., Pertwee, R. G., Stevenson, L. A., Griffin, G., … Mechoulam, R. (1992). Isolation and structure of a brain constituent that binds to the cannabinoid receptor. *Science*, *258*, 1946–1949.

Donvito, G., Wilkerson, J. L., Damaj, M. I., & Lichtman, A. H. (2016). Palmitoylethanolamide reverses paclitaxel-induced allodynia in mice. *The Journal of Pharmacology and Experimental Therapeutics*, *359*, 310–318.

Fegley, D., Gaetani, S., Duranti, A., Tontini, A., Mor, M., Tarzia, G., & Piomelli, D. (2005). Characterization of the fatty acid amide hydrolase inhibitor cyclohexyl carbamic acid 3′-carbamoyl-biphenyl-3-yl ester (URB597): Effects on anandamide and oleoylethanolamide deactivation. *The Journal of Pharmacology and Experimental Therapeutics*, *313*, 352–358.

Fields, H. L. (2011). The doctor's dilemma: Opiate analgesics and chronic pain. *Neuron*, *69*, 591–594.

Fu, J., Gaetani, S., Oveisi, F., Lo Verme, J., Serrano, A., Rodriguez De Fonseca, F., … Piomelli, D. (2003). Oleylethanolamide regulates feeding and body weight through activation of the nuclear receptor PPAR-α. *Nature*, *425*, 90–93.

Gobbi, G., Bambico, F. R., Mangieri, R., Bortolato, M., Campolongo, P., Solinas, M., … Piomelli, D. (2005). Antidepressant-like activity and modulation of brain monoaminergic transmission by blockade of anandamide hydrolysis. *Proceedings of the National Academy of Sciences of the United States of America*, *102*, 18,620–18,625.

de Guglielmo, G., Kallupi, M., Scuppa, G., Stopponi, S., Demopulos, G., Gaitanaris, G., & Ciccocioppo, R. (2014). Analgesic tolerance to morphine is regulated by PPARγ. *British Journal of Pharmacology*, *171*, 5407–5416.

Harding, S. D., Sharman, J. L., Faccenda, E., Southan, C., Pawson, A. J., Ireland, S., … NC-IUPHAR. (2018). The IUPHAR/BPS guide to pharmacology in 2018: Updates and expansion to encompass the new guide to immunopharmacology. *Nucleic Acids Research*, *46*, D1091–D1106. https://doi.org/10.1093/nar/gkx1121

Hasanein, P., & Ghafari-Vahed, M. (2016). Fatty acid amide hydrolase inhibitor URB597 prevented tolerance and cognitive deficits induced by chronic morphine administration in rats. *Behavioural Pharmacology*, *27*, 37–43.

Hayhurst, C. J., & Durieux, M. E. (2016). Differential opioid tolerance and opioid-induced hyperalgesia: A clinical reality. *Anesthesiology*, *124*, 483–488.

Heinzen, E. L., & Pollack, G. M. (2004). The development of morphine antinociceptive tolerance in nitric oxide synthase-deficient mice. *Biochemical Pharmacology*, *67*, 735–741.

Hosohata, Y., Quock, R. M., Hosohata, K., Makriyannis, A., Consroe, P., Roeske, W. R., & Yamamura, H. I. (1997). AM630 antagonism of cannabinoid-stimulated [^{35}S]GTPγS binding in the mouse brain. *European Journal of Pharmacology*, *321*, R1–R3.

Hussain, Z., Uyama, T., Tsuboi, K., & Ueda, N. (2017). Mammalian enzymes responsible for the biosynthesis of *N*-acylethanolamines. *Biochimica et Biophysica Acta - Molecular and Cell Biology of Lipids*, *1862*, 1546–1561.

Ibrahim, M. M., Porreca, F., Lai, J., Albrecht, P. J., Rice, F. L., Khodorova, A., … Malan, T. P. Jr. (2005). CB2 cannabinoid receptor activation produces antinociception by stimulating peripheral release of endogenous opioids. *Proceedings of the National Academy of Sciences of the United States of America*, *102*, 3093–3098.

Inturrisi, C. E. (2002). Clinical pharmacology of opioids for pain. *The Clinical Journal of Pain*, *18*, S3–S13.

Kaczocha, M., Glaser, S. T., Chae, J., Brown, D. A., & Deutsch, D. G. (2010). Lipid droplets are novel sites of *N*-acylethanolamine inactivation by fatty acid amide hydrolase-2. *The Journal of Biological Chemistry*, *285*, 2796–2806.

Kilkenny, C., Browne, W., Cuthill, I. C., Emerson, M., Altman, D. G., & NC3Rs Reporting Guidelines Working Group. (2010). Animal research: Reporting in vivo experiments: The ARRIVE guidelines. *British Journal of Pharmacology*, *160*, 1577–1579.

Lan, R., Liu, Q., Fan, P., Lin, S., Fernando, S. R., McCallion, D., … Makriyannis, A. (1999). Structure-activity relationships of pyrazole derivatives as cannabinoid receptor antagonists. *Journal of Medicinal Chemistry*, *42*, 769–776.

LoVerme, J., La Rana, G., Russo, R., Calignano, A., & Piomelli, D. (2005). The search for the palmitoylethanolamide receptor. *Life Sciences*, *77*, 1685–1698.

LoVerme, J., Russo, R., La Rana, G., Fu, J., Farthing, J., Mattace-Raso, G., … Piomelli, D. (2006). Rapid broad-spectrum analgesia through activation of peroxisome proliferator-activated receptor-α. *The Journal of Pharmacology and Experimental Therapeutics*, *319*, 1051–1061.

Maccarrone, M. (2017). Metabolism of the endocannabinoid anandamide: Open questions after 25 years. *Frontiers in Molecular Neuroscience*, *10*, 166.

Maduna, T., Audouard, E., Dembele, D., Mouzaoui, N., Reiss, D., Massotte, D., & Gaveriaux-Ruff, C. (2018). Microglia express μ opioid receptor: Insights from transcriptomics and fluorescent reporter mice. *Frontiers in Psychiatry*, *9*, 726.

Magotti, P., Bauer, I., Igarashi, M., Babagoli, M., Marotta, R., Piomelli, D., & Garau, G. (2015). Structure of human *N*-acylphosphatidylethanolamine-hydrolyzing phospholipase D: Regulation of fatty acid ethanolamide biosynthesis by bile acids. *Structure*, *23*, 598–604.

Mamiya, T., Noda, Y., Ren, X., Nagai, T., Takeshima, H., Ukai, M., & Nabeshima, T. (2001). Morphine tolerance and dependence in the nociceptin receptor knockout mice. *Journal of Neural Transmission (Vienna)*, *108*, 1349–1361.

Mazzola, C., Medalie, J., Scherma, M., Panlilio, L. V., Solinas, M., Tanda, G., … Yasar, S. (2009). Fatty acid amide hydrolase (FAAH) inhibition enhances memory acquisition through activation of PPAR-α nuclear receptors. *Learning & Memory*, *16*, 332–337.

McKinney, M. K., & Cravatt, B. F. (2005). Structure and function of fatty acid amide hydrolase. *Annual Review of Biochemistry*, *74*, 411–432.

Mor, M., Rivara, S., Lodola, A., Plazzi, P. V., Tarzia, G., Duranti, A., … Piomelli, D. (2004). Cyclohexylcarbamic acid 3′- or 4′-substituted biphenyl-3-yl esters as fatty acid amide hydrolase inhibitors: Synthesis, quantitative structure-activity relationships, and molecular modeling studies. *Journal of Medicinal Chemistry*, *47*, 4998–5008.

Moreno-Sanz, G., Duranti, A., Melzig, L., Fiorelli, C., Ruda, G. F., Colombano, G., … Piomelli, D. (2013). Synthesis and structure-activity relationship studies of *O*-biphenyl-3-yl carbamates as peripherally restricted fatty acid amide hydrolase inhibitors. *Journal of Medicinal Chemistry*, *56*, 5917–5930.

Morgan, M. M., & Christie, M. J. (2011). Analysis of opioid efficacy, tolerance, addiction and dependence from cell culture to human. *British Journal of Pharmacology*, *164*, 1322–1334.

Nguyen, T. L., Nam, Y. S., Lee, S. Y., Kim, H. C., & Jang, C. G. (2010). Effects of capsazepine, a transient receptor potential vanilloid type 1 antagonist, on morphine-induced antinociception, tolerance, and dependence in mice. *British Journal of Anaesthesia*, *105*, 668–674.

Niiyama, Y., Kawamata, T., Yamamoto, J., Furuse, S., & Namiki, A. (2009). SB366791, a TRPV1 antagonist, potentiates analgesic effects of systemic morphine in a murine model of bone cancer pain. *British Journal of Anaesthesia*, *102*, 251–258.

Nozaki, C., Markert, A., & Zimmer, A. (2015). Inhibition of FAAH reduces nitroglycerin-induced migraine-like pain and trigeminal neuronal hyperactivity in mice. *European Neuropsychopharmacology*, *25*, 1388–1396.

Panlilio, L. V., Thorndike, E. B., Nikas, S. P., Alapafuja, S. O., Bandiera, T., Cravatt, B. F., … Justinova, Z. (2016). Effects of fatty acid amide hydrolase (FAAH) inhibitors on working memory in rats. *Psychopharmacology*, *233*, 1879–1888.

Piomelli, D., Hohmann, A. G., Seybold, V., & Hammock, B. D. (2014). A lipid gate for the peripheral control of pain. *The Journal of Neuroscience*, *34*, 15,184–15,191.

Piomelli, D., & Sasso, O. (2014). Peripheral gating of pain signals by endogenous lipid mediators. *Nature Neuroscience*, *17*, 164–174.

Piomelli, D., Tarzia, G., Duranti, A., Tontini, A., Mor, M., Compton, T. R., … Putman, D. (2006). Pharmacological profile of the selective FAAH inhibitor KDS-4103 (URB597). *CNS Drug Reviews*, *12*, 21–38.

Richner, M., Jager, S. B., Siupka, P., & Vaegter, C. B. (2017). Hydraulic extrusion of the spinal cord and isolation of dorsal root ganglia in rodents. *Journal of Visualized Experiments*. https://doi.org/10.3791/55226

Rock, E. M., Moreno-Sanz, G., Limebeer, C. L., Petrie, G. N., Angelini, R., Piomelli, D., & Parker, L. A. (2017). Suppression of acute and anticipatory nausea by peripherally restricted fatty acid amide hydrolase inhibitor in animal models: Role of PPARα and CB1 receptors. *British Journal of Pharmacology*, *174*, 3837–3847.

Roques, B. P., Fournie-Zaluski, M. C., & Wurm, M. (2012). Inhibiting the breakdown of endogenous opioids and cannabinoids to alleviate pain. *Nature Reviews. Drug Discovery*, *11*, 292–310.

Russo, R., Loverme, J., La Rana, G., Compton, T. R., Parrott, J., Duranti, A., … Piomelli, D. (2007). The fatty acid amide hydrolase inhibitor URB597 (cyclohexylcarbamic acid 3′-carbamoylbiphenyl-3-yl ester) reduces neuropathic pain after oral administration in mice. *The Journal of Pharmacology and Experimental Therapeutics*, *322*, 236–242.

Sagar, D. R., Kendall, D. A., & Chapman, V. (2008). Inhibition of fatty acid amide hydrolase produces PPAR-α-mediated analgesia in a rat model of inflammatory pain. *British Journal of Pharmacology*, *155*, 1297–1306.

Sasso, O., Bertorelli, R., Bandiera, T., Scarpelli, R., Colombano, G., Armirotti, A., … Piomelli, D. (2012). Peripheral FAAH inhibition causes profound antinociception and protects against indomethacin-induced gastric lesions. *Pharmacological Research*, *65*(5), 553563. https://doi.org/10.1016/j.phrs.2012.02.012

Sasso, O., Pontis, S., Armirotti, A., Cardinali, G., Kovacs, D., Migliore, M., … Piomelli, D. (2016). Endogenous *N*-acyl taurines regulate skin wound healing. *Proceedings of the National Academy of Sciences of the United States of America*, *113*, E4397–E4406.

Slivicki, R. A., Saberi, S. A., Iyer, V., Vemuri, V. K., Makriyannis, A., & Hohmann, A. G. (2018). Brain-permeant and -impermeant inhibitors of fatty acid amide hydrolase synergize with the opioid analgesic morphine to suppress chemotherapy-induced neuropathic nociception without enhancing effects of morphine on gastrointestinal transit. *The Journal of Pharmacology and Experimental Therapeutics*, *367*, 551–563.

Smith, H. S., & Peppin, J. F. (2014). Toward a systematic approach to opioid rotation. *Journal of Pain Research*, *7*, 589–608.

Tonner, P. H. (2017). Additives used to reduce perioperative opioid consumption 1: α2-agonists. *Best Practice & Research. Clinical Anaesthesiology*, *31*, 505–512.

Tsuboi, K., Uyama, T., Okamoto, Y., & Ueda, N. (2018). Endocannabinoids and related *N*-acylethanolamines: Biological activities and metabolism. *Inflamm Regen*, *38*, 28.

Ueda, N., Tsuboi, K., & Uyama, T. (2013). Metabolism of endocannabinoids and related *N*-acylethanolamines: Canonical and alternative pathways. *The FEBS Journal*, *280*, 1874–1894.

Volkow, N. D., & Collins, F. S. (2017). The role of science in addressing the opioid crisis. *The New England Journal of Medicine*, *377*, 391–394.

Vozella, V., Ahmed, F., Choobchian, P., Merrill, C. B., Zibardi, C., Tarzia, G., … Piomelli, D. (2019). Pharmacokinetics, pharmacodynamics and safety studies on URB937, a peripherally restricted fatty acid amide hydrolase inhibitor, in rats. *The Journal of Pharmacy and Pharmacology*, *71*, 1762–1773.

Wei, D., Lee, D., Cox, C. D., Karsten, C. A., Penagarikano, O., Geschwind, D. H., … Piomelli, D. (2015). Endocannabinoid signaling mediates oxytocin-driven social reward. *Proceedings of the National Academy of Sciences of the United States of America*, *112*, 14,084–14,089.

Wick, E. C., Grant, M. C., & Wu, C. L. (2017). Postoperative multimodal analgesia pain management with nonopioid analgesics and techniques: A review. *JAMA Surgery*, *152*, 691–697.

Wilkerson, J. L., Ghosh, S., Mustafa, M., Abdullah, R. A., Niphakis, M. J., Cabrera, R., … Lichtman, A. H. (2017). The endocannabinoid hydrolysis inhibitor SA-57: Intrinsic antinociceptive effects, augmented morphine-induced antinociception, and attenuated heroin seeking behavior in mice. *Neuropharmacology*, *114*, 156–167.

Woodhams, S. G., Chapman, V., Finn, D. P., Hohmann, A. G., & Neugebauer, V. (2017). The cannabinoid system and pain. *Neuropharmacology*, *124*, 105–120.

Xu, H. E., Stanley, T. B., Montana, V. G., Lambert, M. H., Shearer, B. G., Cobb, J. E., … Stimmel, J. B. (2002). Structural basis for antagonist-mediated recruitment of nuclear co-repressors by PPARα. *Nature*, *415*, 813–817.

How to cite this article: Fotio Y, Palese F, Guaman Tipan P, Ahmed F, Piomelli D. Inhibition of fatty acid amide hydrolase in the CNS prevents and reverses morphine tolerance in male and female mice. *Br J Pharmacol*. 2020;177:3024–3035. https://doi.org/10.1111/bph.15031